Available online at www.sciencedirect.com

ScienceDirect

Procedia Engineering 110 (2015) 2 – 7

Procedia Engineering

www.elsevier.com/locate/procedia

4th International Conference on Tissue Engineering, ICTE2015

Fibre Reinforcement in Living Cells: a Preliminary Study of the F-actin Filaments

João Ferreira[a], Marco Parente[a], Renato Natal[a]

[a]*INEGI, FEUP- Faculdade de Engenharia da Universidade do Porto, Portugal*

Abstract

Cells are continuously exposed to physical stresses and strains from the Extracellular Matrix (ECM), thus, refining through numerical simulations the in vitro conditions during the cultures, may likely promote adequate tissue growth and remodelling [1].

This paper describes a simplified three-dimensional constitutive model of the mechanical behaviour of the living cells. The necessary continuum mechanics background is skipped, along with derivations of the stress and spatial elasticity tensors for a transversely isotropic and hyperelastic material. The particular form of the strain energy proposed by Weiss [2] is used to describe the family of fibers. Also, the implementation of hyperelastic materials resorting the commercial finite-element-software Abaqus is discussed.

Numerical examples are presented that demonstrate the utility and effectiveness of this approach. More specifically, homogeneous deformations are imposed and the results compared with the analytical solution. Also, the convergence rate is checked for each case. Following, the use of UMAT routines using jacobian material matrices based on the Jaumann rate of Kirchhoff stress tensor ensured quadratic convergence rates.

Peer-review under responsibility of IDMEC-IST

Keywords:

Cell Mechanics, Computational Methods, Hyperelastic Materials, F-actin Network

1. Introduction

Cells sense mechanical stimuli and respond biochemically resorting the mechanotransduction mechanisms. The cells behaviour at bioreactors is highly influenced by the scaffold (material, architecture, cells distribution within, coatings), by the use of trophic factors, and by the mechanical loading profile at bioreactor.

Indeed, capture the mechanical response of an single cell restricted to move through an specific scaffold architecture and subjected to biological and chemical conditions is important to reach design parameters and to establish safety factors into regenerative treatments. The design parameters can be obtained by the prioritization and focus on the biomechanical properties of the native tissues and by identification of the cells mechanisms during the regenerative treatment, bringing success cases in a near future. However, achieve those design parameters is not a trivial task and many challenges still remain regarding: the control of the in vitro cultures in bioreactors, the manufacturing processes

E-mail address: jpsferreira@inegi.up.pt

Peer-review under responsibility of IDMEC-IST
doi:10.1016/j.proeng.2015.07.002

of the scaffolds, and the computational methods to provide frameworks to understand the mechanostransduction processes.

At a first instance, adherent cells encompass a passive nonlinear rheological response [3]. Constitutive hyperelastic models describe the energetic terms of the mechanical behaviour. The strain energy density function (or strain-energy function) correspond to the free Helmholtz free energy of the body undergoing deformation, per its unit volume, and can be expressed uniquely in terms of the principal stretches or in terms of the invariants of the left Cauchy-Green deformation tensor or right Cauchy-Green deformation tensor. Considering imcompressible and isotropic hyperelastic materials, with isothermal behaviour for quasi-static solicitations, the strain-energy function just depends on initial and final state of the deformation history. Ronald Rivlin and Melvin Mooney developed the first hyperelastic models. Later, the Neo-Hookean, Ogden, and Arruda-Boyce elastic solids came out, among others.[4–9]. The strain-energy function is obtained by symmetry, thermodynamic, and energetic considerations. Thus, the set of coefficients of the strain-energy function must be obtained experimentally.

2. Transverserly Isotropic Material

The Neo-Hooke material can be presented in the following form

$$U\left(\bar{I}_1, J\right) = U_{iso}\left(\bar{I}_1\right) + U_J\left(J\right) = C_{10}(\bar{I}_1 - 3) + \frac{1}{D}\left(J-1\right)^2 \tag{1}$$

Considering fibres, the unit vector field $\mathbf{a}_a^0$ in the undeformed configuration that describes the local fiber direction influences the strain energy value for a certain material point. In this case, the strain energy can be expressed as a function of the right Cauchy-Green deformation tensor and the structural tensor $\mathbf{a}_a^0 \otimes \mathbf{a}_a^0$, resulting in a different behavior in the fiber direction [2]

$$U = U\left(\mathbf{C}, \mathbf{a}_a^0 \otimes \mathbf{a}_a^0\right) \tag{2}$$

Weiss et al. [2] suggested a constitutive model that uses a strain energy function of the form

$$U = U_J\left(J\right) + U_{iso}\left(\bar{I}_1, \bar{I}_2\right) + U_f\left(\bar{I}_4\right) \tag{3}$$

The fiber contribution is given by

$$U_f = C3\left(e^{(\bar{I}_4 - 1)} - \bar{I}_4\right) \tag{4}$$

and the ground substance (isotropic) (U_{iso}) and volumetric contributions (U_J) are the same announced for the Neo-Hooke material.

3. Cauchy Stress Tensor and Material Jacobian Matrix

Within the UMAT subroutine, the current Cauchy stress tensor STRESS and the Jacobian matrix of the constitutive model DDSDDE based on the specific strain energy of the material are defined. After the call for the current integration point, the UMAT update the Cauchy stress tensor, the state variables resorting the current state (if there is any dissipative mechanism during the deformation history) and the material Jacobian matrix. For user-defined quasi-incompressible materials the penalty method is usually adopted. However, to guarantee quadratic convergence of the solutions in the underlying Newton-Raphson scheme and in the context of the commercial finite-element-software Abaqus, the particular choice of stress tensor and tangent moduli is prescribed by Abaqus, namely, the consistent tangent moduli must be explicitly calculated based on the Jaumann rate of the Kirchoff stress tensor [10].

The related spatial rate-constitutive equations in form of the Lie derivative of the Kirchhoff stress read

$$\mathcal{L}_v \boldsymbol{\tau} = \mathbf{c}^{\tau} : \mathbf{D} \tag{5}$$

where $\mathbf{c}^{\tau}$ is the spatial elasticity tensor and $\mathbf{D}$ is the symmetric part of the velocity gradient, commonly denoted as the rate of deformation tensor [11].

Formulating in terms of the Jaumann stress rate

$$\overset{\circ}{\boldsymbol{\tau}} = \dot{\boldsymbol{\tau}} - \mathbf{W}\cdot\boldsymbol{\tau} - \boldsymbol{\tau}\cdot\mathbf{W}^T \tag{6}$$

results in

$$\mathcal{L}_v\boldsymbol{\tau} = \overset{\circ}{\boldsymbol{\tau}} - \mathbf{D}\cdot\boldsymbol{\tau} - \boldsymbol{\tau}\cdot\mathbf{D} \tag{7}$$

Relation 5 together with 7 results in

$$\overset{\circ}{\boldsymbol{\tau}} = \overset{\circ}{\mathbf{c}}^{\tau} : \mathbf{D} \text{ with } \overset{\circ}{\mathbf{c}}^{\tau} = \mathbf{c}^{\tau} + \mathbf{I}\overline{\otimes}\boldsymbol{\tau} + \boldsymbol{\tau}\overline{\otimes}\mathbf{I} \tag{8}$$

The corresponding tangent moduli conjugate to the Cauchy stresses $\boldsymbol{\sigma} = J^{-1}\boldsymbol{\tau}$ read

$$\overset{\circ}{\mathbf{c}} = \frac{1}{J}\overset{\circ}{\mathbf{c}}^{\tau} \tag{9}$$

or even

$$\overset{\circ}{\mathbf{c}} = \frac{1}{J}\frac{\partial\overset{\circ}{\boldsymbol{\tau}}}{\partial\mathbf{D}} \tag{10}$$

This fourth order tensor does not generally possess minor symmetry, so, generally only its fully symmetric part is taken into account [10,12].

$$\overset{\circ}{\mathbf{c}}^{sym} = \overset{\circ}{\mathbf{c}} + \frac{1}{2}\left[\mathbf{I}\overline{\otimes}\boldsymbol{\sigma} + \boldsymbol{\sigma}\overline{\otimes}\mathbf{I} + \mathbf{I}\otimes\boldsymbol{\sigma} + \boldsymbol{\sigma}\otimes\mathbf{I}\right] \tag{11}$$

For a purely mechanical system and assuming that the material is elastic, the rate of dissipation in the Clausius-Duhem condition should vanish, which implies that

$$\boldsymbol{\sigma} : \mathbf{D} - \rho\dot{U} = 0 \tag{12}$$

Considering the specific strain energy function U as a function of the determinant of the deformation $J = \det(\mathbf{F})$, the first and second invariants of $\bar{\mathbf{B}}$, the squared of the isochoric stretch of the fibers $\bar{I}_{4,\alpha}$, and of the true strech of the fibers $\lambda_{f,\alpha}$

$$U = U\left(J, \bar{I}_1, \bar{I}_2, \bar{I}_{4,\alpha}, \lambda_{f,\alpha}\right) \tag{13}$$

We can now back to the Clausius-Duhem condition and apply the chain rule. Thus,

$$\boldsymbol{\sigma} : \mathbf{D} = \frac{1}{J}\left[\frac{\partial U}{\partial J}\dot{J} + \frac{\partial U}{\partial \bar{I}_1}\dot{\bar{I}}_1 + \frac{\partial U}{\partial \bar{I}_2}\dot{\bar{I}}_2 + \frac{\partial U}{\partial \bar{I}_{4,\alpha}}\dot{\bar{I}}_{4,\alpha} + \frac{\partial U}{\partial \lambda_{f,\alpha}}\dot{\lambda}_{f,\alpha}\right] \tag{14}$$

Using equation 14 on equations 6 and 10 it is noticed that once the derivatives of U with respect to $\bar{I}_1$, $\bar{I}_2$, $\bar{I}_{4,\alpha}$, and $\lambda_{f,\alpha}$ are explicitly defined, the transversly hyperelastic material with one family of fibers can be derived. The exposed formulae can be applied for any hyperlastic material model, conferring a generalist framework for further developments.

4. Results

The numerical tangent moduli from equation 10 and the Cauchy stress tensor obtained form equation 6 are implemented in Abaqus via UMAT for Neo-Hooke, Mooney-Rivlin, and Ogden ground substances and the fibre-reinforcement proposed by Weiss.

The goal of this example is the validation of the numerical implementation of the FORTRAN code by comparing with the analytical solutions. On this matter, the stress field and the total number of iterations for each time increment used by the solver are registered. In this way, the results are computed for each material model considering 2 distinct

homogeneous load cases, namely: uniaxial tension and equibiaxial. A unique C3D8H element (8-ndode linear, hybrid with constant pressure) of unit length ($L = 1$) is used by imposing the boundary conditions and loads for each homogenous stress state.

The deformed configurations of the element are presented in the Figure 1, where it is verified that the boundary conditions were correctly imposed. For this example, the fibre direction is aligned, at least, with one direction of the applied force.

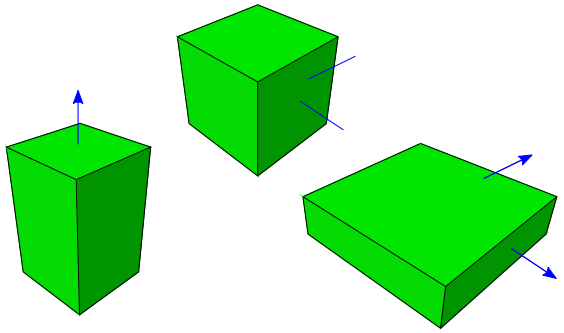

Figure 1: Deformed geometrical configuration for the 2 load cases: uniaxial tension and equibiaxial.

The analytical solution for the Cauchy tensor is obtained by [2]

$$\boldsymbol{\sigma} = p\mathbf{I} + \frac{2}{J}\left[\left(\frac{\partial U}{\partial \bar{I}_1} + \frac{\partial U}{\partial \bar{I}_2}\bar{I}_1\right)\mathbf{B} - \frac{\partial U}{\partial \bar{I}_2}\mathbf{B}^2 + \frac{\partial U}{\partial \bar{I}_4}\bar{I}_4\mathbf{a}_a \otimes \mathbf{a}_a - \frac{1}{3}\left(\frac{\partial U}{\partial \bar{I}_1}\bar{I}_1 + 2\frac{\partial U}{\partial \bar{I}_2}\bar{I}_2 + \frac{\partial U}{\partial \bar{I}_4}\bar{I}_4\right)\mathbf{I}\right] \tag{15}$$

where p is obtained applying the boundary conditions of the problem. The analytical solution where obtained resorting the *Mathematica* software.

Regarding the hyperelastic properties, the coefficients of the strain-energy function are $C_{10} = 10.0$, $C_3 = 100.0$ and $D = 0.0002$.

Figure 2 show the Cauchy stress in the fibre direction and the Relative error (in percentage) for the uniaxial tensile stress state considering the Neo-Hooke (NH) material models as the ground substance. In its turn, Figure 3 and show the Cauchy stress and the Relative error (in percentage) for the equibiaxial stress state.

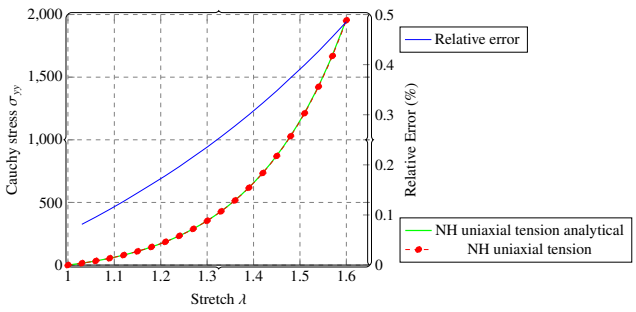

Figure 2: Cauchy stress σ_{yy} and Relative Error (%) as a function of the stretch λ in the y-direction for the uniaxial tensile stress state.

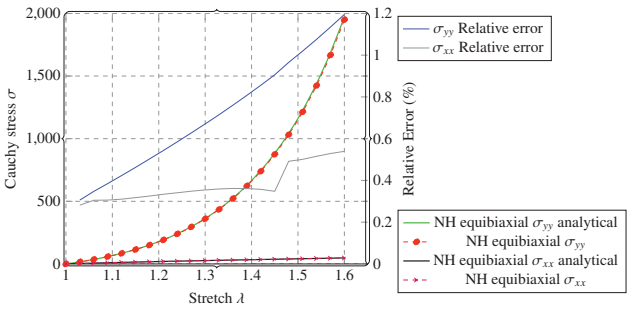

Figure 3: Cauchy stresses and Relative Error (%) as a function of the stretch λ in the y-direction for the equibiaxial tensile stress state.

For both examples, quadratic convergence were ensured. Finally, Figure 4 show qualitatively the structural reinforcement in the fibres direction in the uniaxial tensile state.

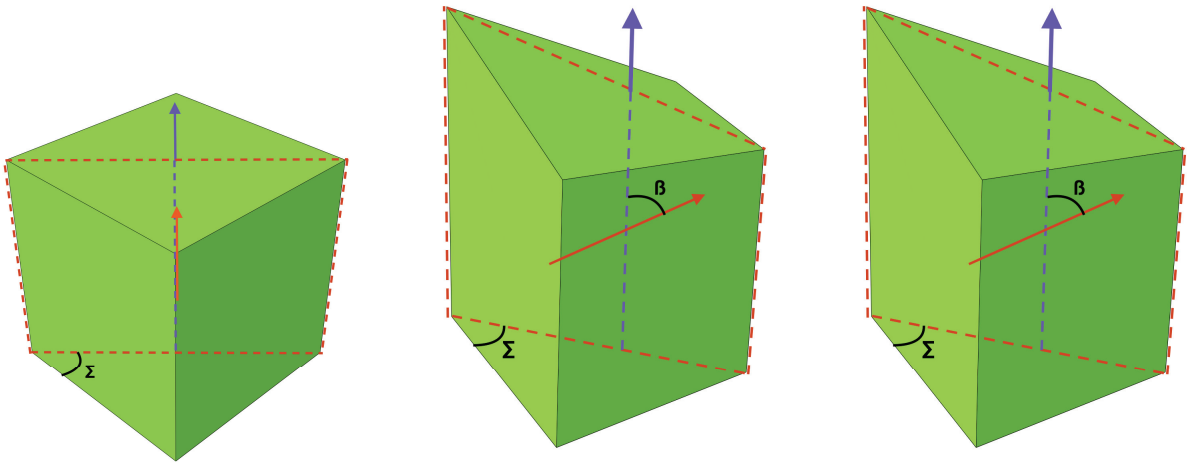

(a) Deformed configuration with aligned fibres

(b) Deformed configuration with misaligned fibres

(c) Deformed configuration with perpendicular fibres

Figure 4: Deformed configuration for differente fibres orientations.

5. Conclusions

The use of UMAT routines using jacobian material matrices based on the Jaumann rate of Kirchhoff stress tensor ensured quadratic convergence rates. The work presented on this paper provides a general framework for further developments regarding the material behaviour of the living cells.

For future works, the fibers contribution should be modified to capture more accuraterely the f-actin network behavior. In fact, based on the results of the mechanical experimental tests, the active behaviour related to the polymerisation and phosphorization of the actin filaments have a crucial role on the overall mechanical response [1].

Acknowledgements

The authors acknowledge the funding of the project UID/EMS/50022/2013, from Fundação da Ciência e Tecnologia, Portugal and to the project "Biomechanics: contributions to the healthcare", reference NORTE-07-0124-FEDER-000035 co-financed by Programa Operacional Regional do Norte (ON.2 – O Novo Norte), through the Fundo Europeu de Desenvolvimento Regional (FEDER).

References

[1] M. L. Rodriguez, B. T. Graham, L. M. Pabon, S. J. Han, C. E. Murry, N. J. Sniadecki, Measuring the Contractile Forces of Human Induced Pluripotent Stem Cell-Derived Cardiomyocytes With Arrays of Microposts, Journal of Biomechanical Engineering 136 (2014) 051005.
[2] J. Weiss, Finite element implementation of incompressible, transversely isotropic hyperelasticity, Computer Methods in Applied Mechanics and Engineering 135 (1996) 107–128.
[3] G. A. Holzapfel, R. W. Ogden, Biomechanical Modelling at the Molecular, Cellular and Tissue Levels, Springer Science & Business Media, 2009.
[4] R. S. Rivlin, A. G. Thomas, Large Elastic Deformations of Isotropic Materials. VIII. Strain Distribution around a Hole in a Sheet, Philosophical Transactions of the Royal Society of London. Series A 243 (1951) 289–298.
[5] R. S. Rivlin, Large Elastic Deformations of Isotropic Materials. IV. Further Developments of the General Theory, Philosophical Transactions of the Royal Society of London. Series A. Mathematical and Physical Sciences 241 (1948) 379–397.
[6] R. S. Rivlin, Large Elastic Deformations of Isotropic Materials. VI. Further Results in the Theory of Torsion, Shear and Flexure, Philosophical Transactions of the Royal Society of London. Series A. Mathematical and Physical Sciences 242 (1949) 173–195.
[7] R. S. Rivlin, Large Elastic Deformations of Isotropic Materials. V. The Problem of Flexure, in: Proceedings of the Royal Society of London. Series A, 1949, pp. 463–473.
[8] R. S. Rivlin, Large Elastic Deformations of Isotropic Materials. I. Fundamental Concepts, Philosophical Transactions of the Royal Society of London. Series A. Mathematical and Physical Sciences 240 (1948) 459–490.
[9] R. S. Rivlin, D. W. Saunders, Large Elastic Deformations of Isotropic Materials. VII. Experiments on the Deformation of Rubber, Philosophical Transactions of the Royal Society of London. Series A 243 (1951) 251–288.
[10] E. Stein, G. Sagar, Convergence behavior of 3D finite elements for Neo-Hookean material, Engineering Computations 25 (2008) 220–232.
[11] W. Sun, E. L. Chaikof, M. E. Levenston, Numerical Approximation of Tangent Moduli for Finite Element Implementations of Nonlinear Hyperelastic Material Models, Journal of Biomechanical Engineering 130 (2008) 061003.
[12] J. C. Simo, T. J. R. Hughes, Computational Inelasticity, Springer, 2013.